SIMULTANEOUS IR AND VISIBLE LIGHT MEASUREMENTS OF THE SOLAR GRANULATION

S. KEIL
U. S. Air Force Phillips Laboratory, Sunspot, NM 88349, U.S.A.
J. KUHN and H. LIN
Michigan State University, East Lansing, MI 48824, U.S.A.
and
K. REARDON
Department of Astronomy, Williams College, Williamstown, MA 01267, U.S.A.

Abstract. Movies of the solar granulation were made simultaneously at 5575 Å and 1.64 μm using the Vacuum Tower Telescope at NSO/SP. A 128 x 128 HgCdTe array was used in the infrared and an RCA 504 CCD in the visible. From the movies, we determine and compare statistical properties of the granulation and seeing conditions.

Key words: convection – infrared: stars – Sun: granulation

1. Introduction

The near infrared spectrum at 1.64 μm offers several advantages for observing the solar granulation. The effects of atmospheric seeing are reduced (the Fried parameter, r_0, which scales as $\lambda^{6/5}$, increases by a factor of 3.5), and since the solar opacity reaches a minimum near 1.64 μm, we see deeper into the solar atmosphere where the granulation is a more dominant effect. (Keil, 1980, Koutchmy, 1988). One difficulty of observing at the longer wavelength is that the granular contrast is reduced. Computations show this reduction to be a factor of $\sim$2 at 1.64 μm (Stein, 1992). Another difficulty is that the angular resolution of the telescope is reduced by a factor of $\sim$3. Although 1.64 μm radiation is formed only 30-40 km below the 5575 Å radiation, the convective heat flux decreases very rapidly with height between these two layers (Bray *et. al.*, 1984) and thus, IR observations can provide a more useful upper boundary condition for models of small-scale solar convection than do observations at visible wavelengths. The effects of the 5-minute oscillations are also greatly reduced at the deeper layer (Koutchmy, 1988) and the granular field is more easily observed.

Turon and Léna (1973) made one of the earliest attempts to measure the solar granulation in the opacity minimum region. They used a linear array and obtained two dimensional images by scanning the sun. In addition, they made center-to-limb photometric scans. While the photometric scans produced results on the center to limb variation of the granular contrast, the imaging was not of sufficient quality to derive properties of the granules. Koutchmy (1988) used a two dimensional IR vidicon equipped with a video digitizer to make movies of the granulation at 1.75 μm. He recorded white light images using a conventional video camera and a VCR at the same time. Because of the non-uniform response of the IR vidicon and the eight bit limitation of the A/D in the video digitizer, he made only qualitative studies of the granulation. He found that the IR granules exhibited a bi-modal intensity distribution and that their lifetimes are shorter in the IR (3.5 min vs. 6 min).

D. M. Rabin et al. (eds.), Infrared Solar Physics, 251–257.

https://doi.org/10.1017/S0074180900124490 Published online by Cambridge University Press

We take advantage of improvements in IR arrays and CCD cameras to simultaneously measure the granules at IR and visible wavelengths and obtain more quantitative properties. In Section 2 we describe the observations. In Section 3 statistical properties of the seeing are discussed and in Section 4 properties of the granules are compared as observed in the two wavelength bands.

2. Observations

Observations were made at the center of the solar disk using the NSO/SP Vacuum Tower Telescope (VTT) on 15 Oct 1990. The beam from the VTT was split between the Universal Birefringent Filter (UBF), which was alternately tuned to 5575 Å (continuum) and 5576.09 Å (core of the Fe I 5576 line) with a 1/8-Å bandpass, and the IR array, which was fed using a 2800Å FWHM filter centered at 1.64 μm. The CCD camera used with the UBF had 300 × 240 pixels, each 16 × 20 μm^2, corresponding to 0.09″ × 0.11″ pixels on the sun, and a field of view of 27″ × 26″. The exposure time was 90 ms and the cadence was one continuum and one line center image every 8 s. The IR array has 128 × 128 pixels, each 60 × 60 μm^2, corresponding to 0.2″ × 0.2″ pixels and a field of view of 26″ × 26″. The exposure time was 1.5 s and the cadance was one image every 4 s. The results presented below were obtained from the first 55 minutes of data taken from a three hour observing sequence. This time period corresponded to the most stable seeing conditions, thus alleviating some of the differences caused by exposure time.

From the raw observations, we produced a 400 frame movie in the continuum at 5575 Å and an 800 frame movie at 1.64 μm. Each movie was then correlation tracked to remove gross motions, destretched to remove differential motions, and finally, passed through a sub-sonic filter to remove the effects of the 5 minute oscillations.

A side by side movie was produced to visually assess the quality of the data. Watching the movie, one gets a distinct impression that seeing conditions are more stable in the IR. Granular evolution is easier to follow in the IR, although when you freeze the movie on any particular frame, it is easy to draw a one to one correspondence between features in the visible and IR. We quantify these impression in the next section.

3. Atmospheric Seeing at 5575 Å and 1.64 μm

We have looked at several properties of the data that are related to atmospheric seeing. These include the amount of image motion, the rms variance of the intensity contrast, and the spatial scale of the data determined from the spatial autocorrelation function of individual images.

As the images were correlation tracked, the values of the x and y displacements needed to align the images were stored. The maximum displacements at 5575 Å were $\Delta x = \pm 0.5''$ and $\Delta y = \pm 0.6''$, with a variance of $\sigma_x = 0.15''$ and $\sigma_y = 0.20''$, while at 1.64 μm, $\Delta x = \pm 0.35''$ and $\Delta y = \pm 0.40''$, $\sigma_x = 0.10''$, and $\sigma_y = 0.14''$. Dispersion plots between the fluctuations at 5575 Å and 1.64 μm showed the displacements were not well correlated, probably owing to the difference in

https://doi.org/10.1017/S0074180900124490 Published online by Cambridge University Press

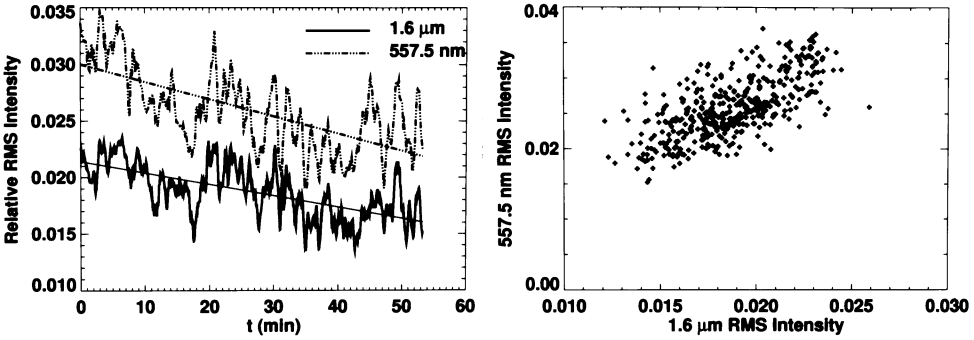

Fig. 1. The panel on the left shows the normalized rms intensity fluctuations observed at 5575 Å and at 1.64 μm. The right hand panel shows the dispersion between the rms values at 5575 Å and 1.64 μm.

exposure times.

The images were destretched by local correlation tracking on a grid of $\sim 2''$ boxes against a reference image that was obtained from a one minute temporal running mean of the data. For each image we stored the displacement at each grid point required to destretch the images. From these displacements, an average displacement was generated for each image and then for the entire time sequence. The mean displacements at 5575 Å and 1.64 μm were $\Delta r = 0.065''$ and $\Delta r = 0.035''$ respectively.

Figure 1a plots the normalized rms intensity fluctuations of each image over the 55 min observing run. The quality of the seeing decreases with time over the 55 minutes. The rms fluctuations observed in the visible and IR track fairly well. Figure 1b shows the dispersion relationship between the two wavelengths. The data has not been corrected for optical or atmospheric transfer functions. If the IR data is corrected for the expected factor of two reduction in contrast at 1.64 μm, we are seeing greater contrast in the IR than in the visible, before correction for atmospheric and instrumental effects. Figure 2 shows spatial autocorrelation functions at the two wavelengths averaged over the 55 min time sequence. The half width at half maximum of the autocorrelation functions gives an estimate of the features sizes being resolved. These widths are 390 km at 1.64 μm compared to the 316 km cutoff of the VTT and 460 km at 5575 Å compared to the 110 km (diffraction) cutoff of the VTT. Thus we are resolving features nearer the telescope cutoff at 1.64 μm than at 5575 Å, in spite of the longer exposures and reduced telescope resolution. This would indicate substantially better seeing conditions at 1.64 μm.

The results for the image motion and correlation tracking displacements can be partially explained by the difference in exposure times. The longer exposures in the IR tend to smear out the atmospherically induced large scale and differential image motions. Thus on the average, we find smaller displacements in the IR. However, these same effects would tend to smear the granules and reduce their contrast in

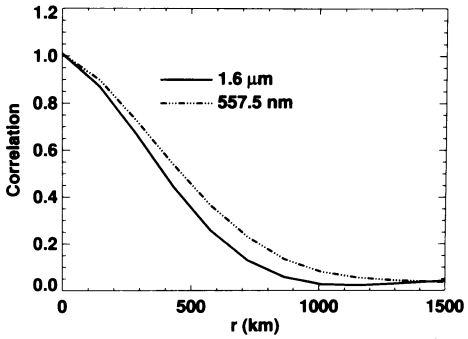

Fig. 2. Mean spatial autocorrelation functions plotted for 1.64 μm and 5575 Å. The autocorrelation of each image was computed as a function of x and y, azimuthally averaged to obtain the radial dependence, and then averaged over time to get the mean functions shown here.

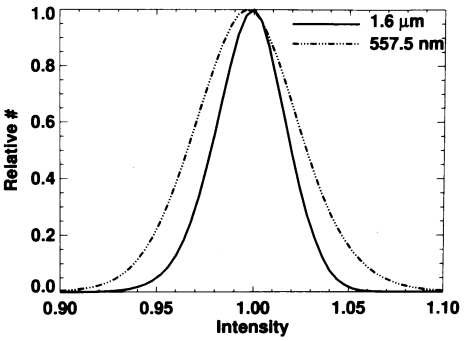

Fig. 3. Histograms of the intensity fluctuations, averaged over the first 15 minutes of data.

the IR and increase the width of the autocorrelation function. Since we are seeing near diffraction limited data in the IR, we conclude that the seeing has less effect on the IR observations.

4. Properties of the Granules at 1.64 μm and 5575 Å

Figure 3 shows intensity histograms, at the two wavelengths, obtained by computing individual histograms for each image in the first 15 minutes of data (the period exhibiting the highest rms intensity fluctuations, see Figure 1) and then averaging the histograms. The distributions are both skewed very slightly to darker values (in

https://doi.org/10.1017/S0074180900124490 Published online by Cambridge University Press

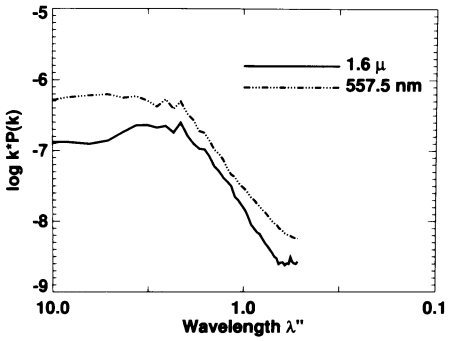

Fig. 4. Radial spatial power spectra, averaged over the 55 min observing sequence.

agreement with the findings of Keil, 1977 and Pravdjuk *et al.*, 1974. We do not see strong evidence for a bimodal distribution as reported by Koutchmy (1988). Seeing could play a role in causing our distribution to be more symmetrical, although our observed rms at 1.64 μm is slightly higher than his observed values at 1.75 μm. The distributions give a ratio of bright to dark elements of 0.88 in the visible and 0.89 in the IR.

Measuring the size and spatial distribution of the solar granulation is extremely difficult and algorithm dependent (Title *et al.*, 1989, Roudier and Muller, 1987). Some of the algorithms that have been used include spatial power spectra and auto-correlations (Deubner and Mattig, 1975), fractal dimensions (Roudier and Muller, 1987), and granule center and lane finding algorithms (*cf.* Title *et al.*). Rather than evaluating the techniques, we compare differences between the IR and visible data. We again emphasize that no corrections for transfer functions have been applied to the data.

Figure 4 compares the spatial power of the intensity fluctuations (as a function of radial wavenumber) at the two wavelengths. The spectra have been averaged over the 55 minute observing run. The power spectra in the IR and visible behave similarly at high wavenumber, corresponding to wavelengths from about 3″ down to the telescope cutoff. This portion of the spectra appears to follow a power law. At low wavenumbers, the IR spectra shows a decrease in power, probably due to the diminished fluctuations associated with the 5 min oscillations discussed below. The IR power is smaller at all wavelengths, in agreement with the observed intensity fluctuations. We have also computed the fractal dimension of the granules using the granular locating algorithm described by Newbury and Keil (1990). We find a smooth increase in the fractal dimension from about 1.3 for small granules to 1.9 for the largest granules in both the visible and IR. This is similar to the result Newbury and Keil find for granules observed in the visible.

The temporal power spectrum was computed at each pixel in the array and then averaged over the array to obtain Figure 5a. The 5 min oscillations show up clearly

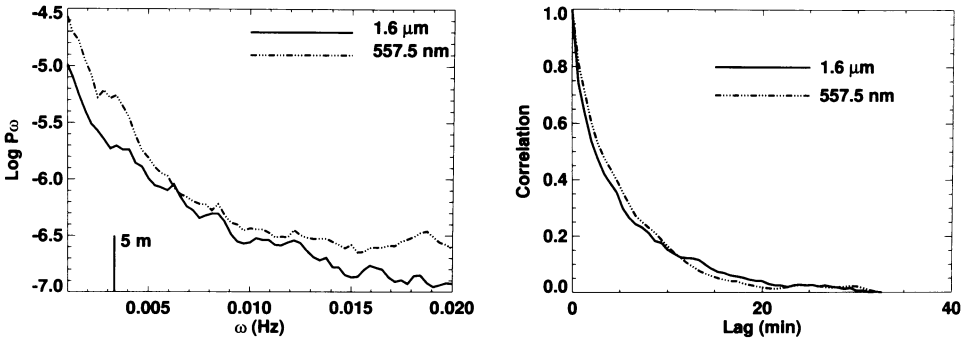

Fig. 5. The left hand panel shows the temporal power spectra averaged over all spatial points. On the right is shown the cross-correlation between the reference frame and subsequent frames. A reference frame was chosen at 40 second intervals and then cross correlated with the subsequent images. These cross correlation functions where then averaged to obtain the mean curves shown in the figure.

in the 5575 Å data but are greatly reduced in the 1.64 μm data. The noise level is substantially reduced in the IR observations, corresponding to a reduction in seeing induced fluctuations. The temporal cross correlation functions are shown in Figure 5b. The correlation between time steps is seen to decrease more rapidly for the IR granulation during the first 10 minutes. This lends support to Koutchmy's (1988) argument that the granules are shorter lived in the opacity minimum region. However, the difference we observe is much smaller than he measures. In addition to the cross correlation functions, we tracked individual granules, starting from a reference frame and then following the granule forward and backward in time until it disappeared. Granules were defined by an algorithm that searched for local maxima. Histograms of the granular lifetimes determined in this manner yield a mean lifetime near 5 minutes in both the IR and visible. We were able to track a few granules for periods near 40 minutes in the IR. None of the visible granules could be tracked longer than 32 minutes.

Acknowledgements

Our thanks to the NSO/SP VTT staff (Dick Mann, Steve Hegwer, and Roy Coulter) for helping obtain the data. The IR array was developed in collaboration with the Astrophysical Research Consortium, with assistance from Michigan State University, the University of Wyoming, and Haverford College.

References

Bray, R. Loughhead, R. and Durrant, C.: 1984, *The Solar Granulation*, Cambridge University Press, 2nd Edition.

Deubner, F. and Mattig, W.: 1975, *Astron. Astrophys.* **45**, 167.

Keil, S.: 1977, *Solar Phys.* **53**, 359.
Keil, S.: 1980, *Astron. Astrophys.* **82**, 144.
Koutchmy, S.: 1988, in J. Stenflo (ed.), 'Solar Photosphere: Structure, Convection and Magnetic Fields', *Proc. IAU Symp.* **138**, 81.
Newbury, J., Keil, S.: 1991, *Bull. Amer. Astron. Soc.* **23**, 1048.
Pravdjuk, L., Karpinsky, V., and Andreiko, A.: 1974, *Soln. Dann.* **2**, 70.
Roudier, T., Muller R.: 1987, *Solar Phys.* **107**, 11.
Stein, R.: 1992, private communication
Title, A., Tarbell, T., Topka, K., Ferguson, S., and Shine, R.: 1987, *Astrophys. J.* **336**, 475.
Turon, P. J. and Léna, P.: 1973, *Solar Phys.* **30**, 3.